

Spin Seebeck effect in thin films of the Heusler compound Co_2MnSi S. Bosu,^{1,*} Y. Sakuraba,¹ K. Uchida,¹ K. Saito,¹ T. Ota,¹ E. Saitoh,^{1,2,3,4} and K. Takanashi¹¹*Institute for Materials Research, Tohoku University, Sendai 980-8577, Japan*²*Advanced Science Research Center, Japan Atomic Energy Agency, Tokai 319-1195, Japan*³*CREST, Japan Science and Technology Agency, Sanbancho, Tokyo 102-0075, Japan*⁴*PRESTO, Japan Science and Technology Agency, Sanbancho, Tokyo 102-0075, Japan*

(Received 19 November 2010; revised manuscript received 3 February 2011; published 16 June 2011)

The recently discovered spin Seebeck effect (SSE) which generates spin voltage due to a temperature gradient in ferromagnets, was systematically studied in half-metallic Heusler compound Co_2MnSi (CMS)/Pt thin films to investigate the effect of spin polarization of ferromagnetic layer on SSE. An epitaxial thin film of CMS with an almost perfect $B2$ -ordered structure was prepared directly on a $\text{MgO}(001)$ substrate. The measurement was performed at room temperature for various temperature differences, $\Delta T = 0\text{--}20$ K between higher ($300\text{ K} + \Delta T$) and lower (300 K) temperature ends along the film. The clear sign reversal of the thermally induced spin voltage due to SSE at the higher and lower temperature ends of the CMS film was detected by means of inverse spin-Hall effect in a Pt wire. The SSE was also investigated in a Py thin film deposited on a $\text{MgO}(001)$ substrate and compared to that with CMS to verify the effect of spin polarization on SSE. Comparable signals of SSE in CMS and Py thin films suggested that thermal excitation of magnons might have more vital effects in SSE than the degree of spin polarization in ferromagnetic metals.

DOI: [10.1103/PhysRevB.83.224401](https://doi.org/10.1103/PhysRevB.83.224401)

PACS number(s): 85.75.-d, 75.76.+j, 75.30.Ds, 72.25.Pn

I. INTRODUCTION

Spintronics, the interface between magnetics and electronics which exploits electron spins, is a new field of research, initiated by the discovery of giant magnetoresistance (GMR) effect^{1,2} in 1988. The basic concept of spintronics is the manipulation of spin current, which provides new effects, new capabilities, and new functionalities.³⁻⁵ However, the creation, manipulation, and detection of spin current⁶ are the main challenges these days. The spin caloritronics that deals with the interplay among spin, charge, and heat currents, is a presently growing branch of spintronics.⁷ The spin analogy of the Seebeck effect, the spin Seebeck effect (SSE), allows one to generate pure spin current and spin voltage by placing a ferromagnetic metal in a temperature gradient. Recently, experimental observation of SSE was reported in several metallic magnets $[\text{Ni}_{81}\text{Fe}_{19}(\text{Py}), \text{Fe}, \text{Ni}]$,⁸⁻¹² where the spin current was detected by means of the inverse spin-Hall effect (ISHE) in a Pt film¹³ ($j_c = D_{\text{ISHE}} j_s \times \sigma$, where, j_c , D_{ISHE} , j_s , and σ represent charge current, coefficient of ISHE, spin current, and spin polarization vector, respectively). The main features of SSE distinctive from other effects [e.g., anomalous Nernst-Ettingshausen effect (ANE)] are (i) a uniform temperature gradient induces a spin voltage that varies along the temperature gradient and (ii) the sign reversal of voltage between higher and lower temperature (HT and LT) ends takes place at the center of the sample due to the change of the direction of spin current polarization vector. At the time of the study by Uchida *et al.*,⁸ the generation of the spin voltage and spin current was considered to be due to the difference in electrochemical potential gradients of two different spins (up and down) of conduction electrons in the ferromagnet in a thermally nonequilibrium situation. Conventionally, SSE was phenomenologically formulated in terms of thermal excitation of conduction electrons.⁹ According to this model, the thermally generated spin current j_s is described as

$$j_s \propto 1 - p_c^2, \quad (1)$$

where $p_c \equiv (\sigma_{\uparrow} - \sigma_{\downarrow})/(\sigma_{\uparrow} + \sigma_{\downarrow})$ denotes spin polarization, with $\sigma_{\uparrow(\downarrow)}$ being spin-dependent electrical conductivity for up (down) spin subbands. This indicates that the thermal spin transport is strongly dependent on the conduction electrons' spin polarization. However, the mystery concerning SSE is how conduction electrons can sustain the spin voltage over several millimeters—unpredictably, much larger than the metallic spin-diffusion length (usually a few nanometers), which has generated vast interest in the thermal aspects of spin transport. In contrast, SSE has been recently discussed in terms of thermal excitation of magnons, i.e., spin waves, where spin polarization is not essential.¹⁴ Therefore, to further verify the mechanism of SSE, more systematic investigations in a wide range of materials are required.

In recent years, the growing development of spintronics has been searching for materials with high Curie temperatures and large spin polarizations. Cobalt-based half-metallic Heusler compounds such as Co_2YZ ($Y = \text{Mn}, \text{Fe}; Z = \text{Si}, \text{Ge}, \text{Al}, \text{etc.}$) have attracted much attention in recent years as prospective candidates¹⁵⁻¹⁷ for spintronics applications. The feature of these materials is that the two spin bands show completely different behavior: the majority spin band is metallic, while the minority spin band exhibits semiconducting behavior with an energy gap at the Fermi level in a $L2_1$ -ordered structure. The Heusler compound Co_2YZ may also grow in the chemically ordered $B2$ [$\text{Co}_2(\text{Y}, \text{Z})$] or disordered [$\text{Co}, \text{Y}, \text{Z}$] structure. Among the half-metallic Heusler compounds, Co_2MnSi (CMS) has already been demonstrated as a useful material for the application in spintronic devices because of the experimental observation of large spin polarization¹⁸ and high tunnel magnetoresistance (TMR) values.¹⁹ Recently, we also reported the enhancement of the resistance change area product (ΔRA) and large magnetoresistance (MR) ratio in current-perpendicular-to-plane giant magnetoresistance (CPP-GMR) in epitaxially grown CMS-based trilayers.²⁰⁻²² Moreover, the bulk spin-asymmetry coefficient β , which corresponds to the

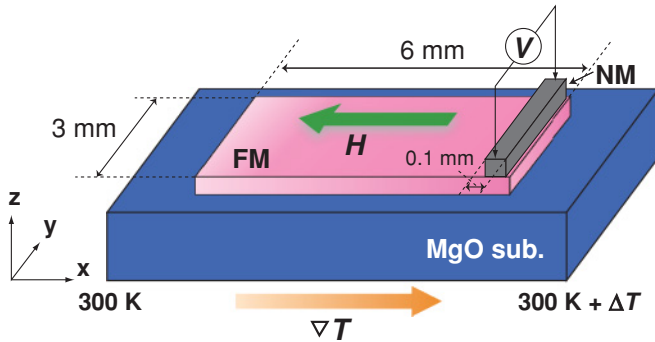


FIG. 1. (Color online) Schematic diagram of the sample used for SSE study.

spin polarization of conduction electrons p_c in a CMS film, was estimated to be ~ 0.9 at low temperature and $0.7\text{--}0.8$ at room temperature (RT) in our very recent study of CPP-GMR.²³ This high β value indicates that p_c in our prepared CMS film is also high even at RT. However, the knowledge of spin caloritronic effects in highly spin polarized Heusler compound based structures is still lacking.²⁴ In case of a material with 100% spin polarization, i.e., $p_c = 1$, according to Eq. (1) there should be no spin current by conduction electrons in the material placed in a temperature gradient. Therefore, it is interesting to investigate the SSE in highly spin polarized materials. The main purpose of this study is to investigate the effect of spin polarization on SSE. In this study, SSE has been investigated in highly spin polarized Heusler compound CMS thin films and compared to that in typical ferromagnetic alloy Py films.

This paper is organized as follows: Section II contains the sample preparation, fabrication and measurement techniques. The experimental results of this study are described in details in Sec. III. In Sec. IV we discuss the experimental observations considering some recent theoretical interpretations and summarize the study.

II. EXPERIMENTAL AND MEASUREMENT

The thin films in this study were prepared by ultrahigh vacuum (UHV) compatible dc sputtering method (base pressure $\sim 1 \times 10^{-7}$ Pa) on a MgO(001) substrate. First, the

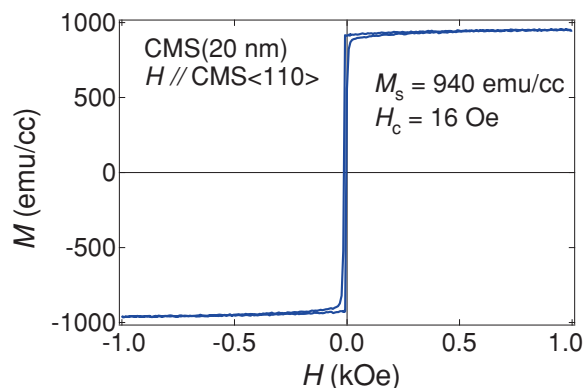


FIG. 2. (Color online) M - H loop of CMS(20 nm) thin film measured along the easy magnetization axis CMS $\langle 110 \rangle$.

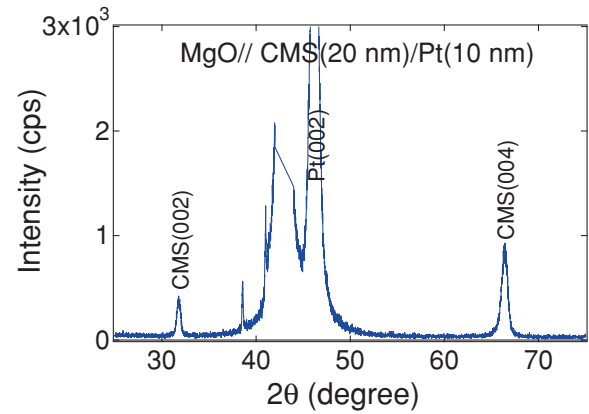


FIG. 3. (Color online) XRD patterns of CMS(20 nm)/Pt(10 nm) thin films.

MgO substrate was annealed at 600°C to achieve a clean and very flat surface. The ferromagnetic (FM) film (FM = CMS, Py) was then deposited at RT. The CMS film was annealed at 500°C for 30 min to enhance the chemical ordering. The epitaxial relationship between MgO and CMS is MgO(001) $\langle 100 \rangle$ /CMS(001) $\langle 110 \rangle$. Finally, a nonmagnetic (NM) metal (NM = Pt, Cu) film of 10 nm thickness was deposited at RT. Figure 1 shows a schematic diagram of the sample for the measurement of SSE fabricated by photolithography and Ar ion milling. The width of FM and the length of NM along the y direction are 3 mm. The length of FM and the width of NM along the x direction are 6 mm and 0.1 mm, respectively.

The SSE has been measured by applying an in-plane external magnetic field H and maintaining a uniform temperature gradient ∇T along the x direction in the plane of the sample, ∇T_x . The voltage was measured at the two ends of NM along the y direction (Fig. 1). The experimental setup and measurement technique are described in detail in a previous paper.¹⁰

The magnetic, structural, and surface characterizations of thin films were made by vibrating sample magnetometer

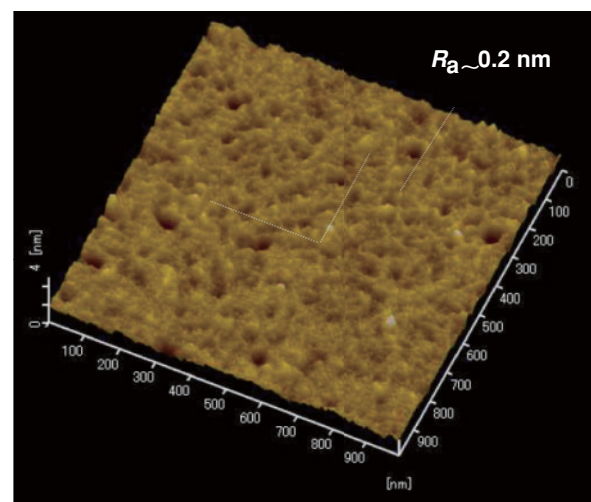


FIG. 4. (Color online) AFM image of CMS(20 nm)/Pt(10 nm) thin films.

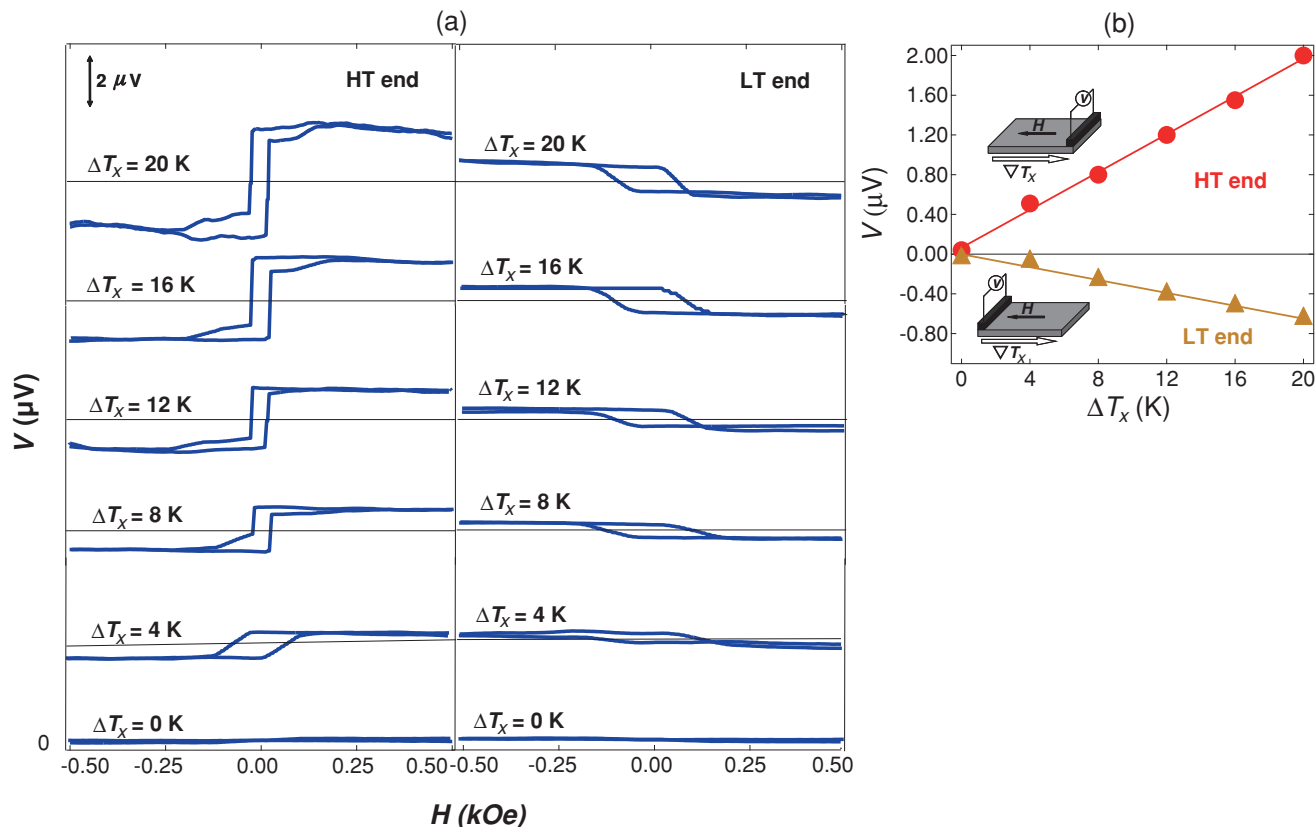


FIG. 5. (Color online) (a) H dependence and (b) ΔT_x dependence of electric voltage V in CMS/Pt sample measured at higher ($300\text{ K} + \Delta T_x$) and lower (300 K) temperature ends.

(VSM), x-ray diffraction (XRD), and atomic force microscopy (AFM), respectively.

III. RESULTS

A. Magnetization and structural characterizations

An M - H loop of a CMS (20 nm) thin film measured along the easy crystallographic axis (CMS(110)) is shown in Fig. 2. The high magnetization value ($M_s \sim 940\text{ emu/cm}^3$) and low coercive field ($H_c \sim 16\text{ Oe}$) indicate good quality of the CMS film. Figure 3 shows the XRD patterns of a θ - 2θ measurement for CMS (20 nm)/Pt(10 nm) sample. The diffractions from only the (001) plane confirm (001)-oriented epitaxial growth of the CMS film. The presence of a strong (002) peak suggests that the CMS film is grown in a $B2$ structure with a high degree of long range ordering. Moreover, in the measurement of the (111) pole figure, the presence of a weak $L2_1$ superlattice (111) peak (not shown here) has also been detected, indicating that the CMS film is grown in a $B2$ -ordered structure with partial $L2_1$ ordering. Theoretical band structure calculations by Picozzi *et al.*¹⁷ predicted that the half metallicity could also be preserved even in a $B2$ -ordered CMS structure. It is important to note here that our CMS films for both the SSE and CPP-GMR studies have been prepared using the same deposition technique. Moreover, magnetization, structural, and chemical ordering characterizations of CMS in both of our studies show almost the same quality of CMS films. Thus, according to our recent experimental investigations of bulk

spin polarization in a CPP-GMR study²³ we can expect a high degree of spin polarization ($p_c > 0.7$) in our CMS films used in this study. Figure 4 shows the average surface roughness R_a in CMS/Pt films measured by AFM. A very small value of R_a ($\sim 0.2\text{ nm}$) implies that the films have very flat surfaces. Therefore, the samples in this study have good magnetic and structural properties as necessary. In addition, the Py films used in this study were grown in a polycrystalline structure with small R_a ($\sim 0.3\text{ nm}$) and the value of M_s and H_c are found to be 840 emu/cm^3 and 20 Oe , respectively. Generally, the experimentally observed degree of spin polarization in Py^{25,26} is relatively small ($p_c \sim 0.25$). Therefore, we can expect that the spin polarization in our CMS films is much higher than that in our Py films [$p_c(\text{CMS}) > p_c(\text{Py})$].

B. SSE in CMS/Pt and Py/Pt thin films

Figures 5(a) and 5(b) show the magnetic field H dependence of measured electric voltage, V , and the temperature difference along x direction, ΔT_x dependence of V at $H = 500$ Oe, respectively, for the CMS/Pt sample. The voltage was measured between the two ends of the Pt wire at the HT and LT ends. The measurements for the HT and LT ends were done by using the same sample, and only by changing the position of Pt wire from the HT to LT end. The magnitude of V increases linearly with ΔT_x at both the HT and LT ends of the sample. The sign of V for finite values of ΔT_x is clearly reversed between the HT and LT ends, which is the main feature of the SSE.⁸ Therefore,

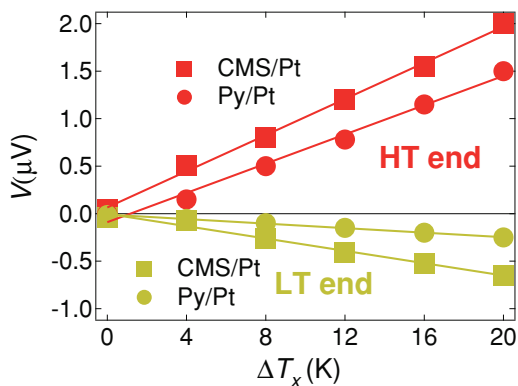


FIG. 6. (Color online) V in CMS/Pt and Py/Pt samples at higher ($300\text{ K} + \Delta T$) and lower (300 K) temperature ends for $\Delta T_x = 0 - 20\text{ K}$.

the sign change of the voltage suggests the presence of SSE in the CMS film. However, asymmetric behavior of magnitude V at HT and LT ends is inconsistent with the feature of SSE observed in Ref. 8.

In addition, in order to compare the behavior of SSE in (Heusler compound) CMS to (typical magnetic alloy) Py, SSE has also been investigated in Py/Pt thin films. Figure 6 shows V as a function of ΔT_x in both the CMS/Pt and Py/Pt samples measured at the HT and LT ends of the sample. A linear relationship between V and ΔT_x is also observed in Py/Pt thin films; moreover, the magnitude of V is comparable to that in CMS/Pt. However, an asymmetric magnitude of V at the HT and LT ends has also been observed in Py/Pt sample. The reproducibility of the V signal has been investigated using several samples (more than five) of each type (CMS/Pt or Py/Pt). A comparable V in CMS/Pt and Py/Pt structures and asymmetric V between HT and LT ends have been detected in both structures.

To investigate the origin of this asymmetric behavior of V , measurements were also performed on single CMS and Py films without the Pt wire, i.e., in the absence of ISHE effect. The temperature gradient along the film plane ∇T_x was maintained the same as in the measurement of SSE, and V was measured along the width of the film between the two ends (y direction) at both the HT and LT ends by applying an external magnetic field H along the film plane, as shown in Fig. 7(a). Figures 7(b) and 7(c) show the voltage measured at the HT and LT ends of the CMS and Py thin films, respectively, as a function of ΔT_x . The same positive sign of V has been observed at both the HT and LT ends and the magnitude of V is proportional to ΔT_x in both the samples. In this geometry, no V signal due to ANE-type effect²⁷ ($E_{ANE} \propto M \times \nabla T$) could be expected as the magnetization of FM film (M), ∇T , and H are in plane. Therefore, it is speculated that the presence of additional perpendicular temperature gradient along z direction, ∇T_z between the FM thin film and the substrate might originate the ANE voltage V_{ANE} . The thermal conductivities k of the metallic CMS and Py films are roughly estimated using the Wiedemann-Franz law ($k_e \rho = \text{constant}$) by measuring the electrical resistivity of thin films. Here, k_e and ρ stand for thermal conductivity and electrical resistivity, respectively. The thermal conductivities of CMS and Py films are estimated to be $11\text{ W m}^{-1}\text{ K}^{-1}$ and $21\text{ W m}^{-1}\text{ K}^{-1}$, respectively, smaller than the thermal conductivity of MgO ($k_{MgO} \sim 48\text{ W m}^{-1}\text{ K}^{-1}$).²⁸ Therefore, the lower thermal conductivity of CMS and Py thin films, compared to MgO substrate, might originate small but finite ∇T_z . However, the evaluation of the value of ΔT_z between substrate and thin film is not straightforward.

To confirm the existence of the contribution of ANE, CMS films with different thicknesses ($t_{CMS} = 5 - 50\text{ nm}$) have been prepared on MgO(001) substrates. The V_{ANE} at the HT end is plotted as a function of ΔT_x for $t_{CMS} = 5 - 50\text{ nm}$ in

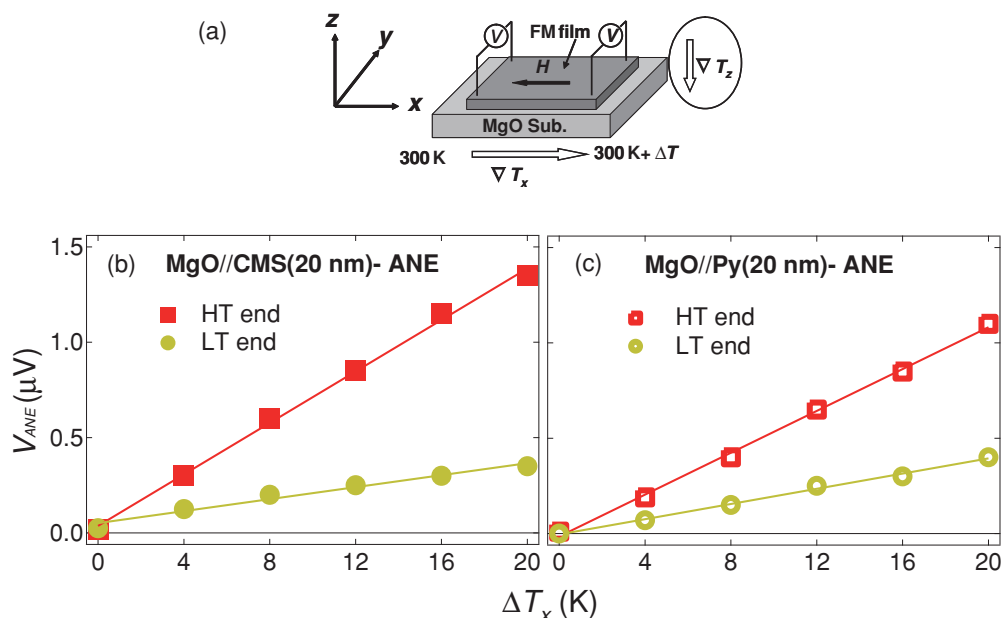


FIG. 7. (Color online) (a) Schematic diagram of the measurement setup of ANE in FM thin films; electric voltage difference of ANE, V_{ANE} as a function of ΔT_x in (b) plain CMS and (c) Py thin films at higher ($300\text{ K} + \Delta T$) and lower (300 K) temperature ends.

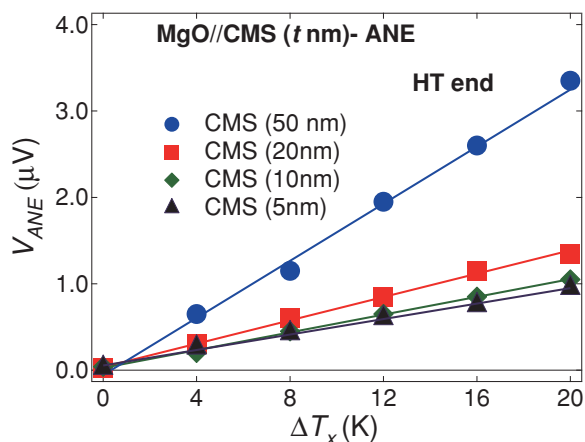


FIG. 8. (Color online) V_{ANE} due to perpendicular ∇T_z as a function of ΔT_x in CMS films for $t_{CMS} = 5\text{--}50$ nm.

Fig. 8. The enhancement of V_{ANE} with t_{CMS} indicates that ΔT_z also increases with t_{CMS} . This observation is evidence of the existence of ANE in the perpendicular direction of CMS films. Thus it could be concluded here that the observed asymmetry of V at the HT and LT ends is caused by the superposition of V_{ANE} which has the same sign at both ends. Moreover, it is not easy to subtract the V_{ANE} from the V signal to make a clear profile of SSE and evaluation of spin Seebeck coefficient in CMS, as the value of ΔT_z is unknown.

Finally, to confirm that the signal observed in CMS(20 nm)/Pt(10 nm) is really due to the ISHE, the Pt wire is replaced by a Cu wire in which no ISHE is expected due to very weak spin-orbit interaction in Cu.²⁹ Figure 9 shows the V observed in CMS(20 nm)/Cu(10 nm) thin films as a function of ΔT_x and compared to that in CMS(20 nm)/Pt(10 nm) thin films. The V observed in CMS/Cu is much weaker than that in CMS/Pt, and the sign of V in CMS/Cu at the HT and LT ends is the same, indicating the absence of ISHE in Cu wire. The observed V in CMS/Cu sample might be induced by the existing ANE in CMS film due to the ∇T_z . However, V_{ANE} that is weaker in CMS/Cu structure than in plain CMS film might be due to the suppression of V_{ANE} by a short circuit effect in Cu wire for high

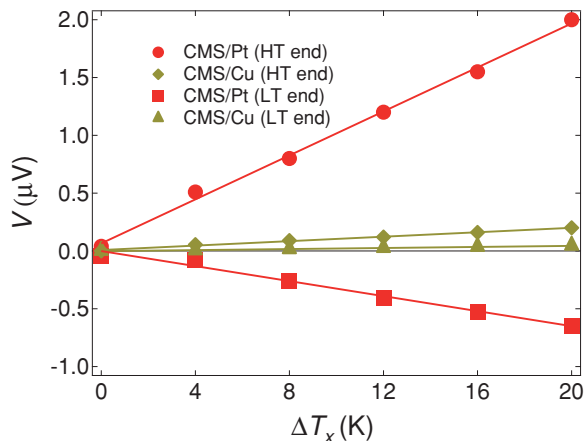


FIG. 9. (Color online) Electric voltage difference V in CMS/Pt and CMS/Cu samples as a function of ΔT_x .

electrical conductivity of Cu. Therefore, the V signal observed in CMS/Pt thin films originates mainly from the SSE in CMS and is detected via ISHE in Pt, indicating an important role of spin-orbit coupling, or ISHE, in the V generation. All of these observations suggest the detection of SSE in full-Heusler alloy CMS.

IV. DISCUSSION AND SUMMARY

In this study, SSE has been observed in a Heusler compound CMS epitaxial film via ISHE in Pt, and the magnitude of the voltage was found to be comparable to that in a magnetic binary alloy Py thin film. No significant difference of SSE has been detected between highly spin polarized and typical ferromagnetic alloys. Very recently, SSE was reported by Uchida *et al.* in magnetic insulator $\text{LaY}_2\text{Fe}_5\text{O}_{12}$ (YIG),³⁰ i.e., in the absence of conduction electrons. The magnitude of V reported in that study is of the same order as observed in Py.⁸ The observed spin voltage was explained by introducing an unconventional nonequilibrium state between the magnetic moments in YIG and the electrons in Pt, and the generation of spin current was considered to be due to the dynamical spin coupling between YIG and Pt. The physical concept of this kind of mechanism is fundamentally different from the static spin injection. Moreover, at the same time SSE was also reported by Jaworski *et al.* in ferromagnetic semiconductor GaMnAs.³¹ The asymmetric V of SSE at hot and cold ends and the presence of V signal in a plain GaMnAs film measured with point contact were also reported in that study. The observed voltage in the plain GaMnAs film³¹ was discussed in terms of the contribution of ANE due to the possibility of the presence of an unavoidable small temperature gradient in GaMnAs film along the sample normal as reported by Pu *et al.*³² All of those observations are consistent with our present results. A very recent semiclassical theory of spin diffusion in a ferromagnetic metal subjected to a temperature gradient by Hatami *et al.*³³ predicted that the spin accumulation cannot persist over distances longer than the metallic spin-diffusion length. They also suggested that a thermally induced spin pumping mechanism due to magnon propagation may explain the spin voltage in ferromagnetic materials. In a successive theoretical study of SSE by Xiao *et al.*¹⁴ considering the thermally driven spin pumping current mechanism, they claimed that the difference between effective magnon and phonon temperatures drives a dc spin current, which can be detected by the ISHE or other techniques. According to their calculation, the SSE is caused by the nonequilibrium between magnon and phonon systems excited by a temperature basis over a ferromagnet, i.e., the SSE originates from the magnon-lattice temperature dependence profile. This model might be suitable for magnetic insulator as the experimental magnon thermalization length λ_{mag} is within the range of calculated λ_{mag} . Although this theory holds for both magnetic insulators and metals, this model has some limitations for ferromagnetic metal as the contribution of conduction electrons is neglected in the calculation. Moreover, the calculated length scale λ_{mag} is about one order smaller than the experimental length scale in Py/Pt.⁸ However, from the present observations in this study and according to the recent theoretical interpretations, it seems that there is no relationship between the degree of spin polarization and SSE

in ferromagnetic metals. Moreover, recent observations of SSE in magnetic insulator³⁰ and semiconductor³¹ indicate that the consideration of thermally excited magnon and phonon propagations would also be essential to clarify the mechanism of SSE.

In conclusion, we have reported the observation of SSE in highly spin polarized Heusler compound CMS/Pt structure, which is comparable to the SSE observed in our conventional ferromagnetic alloy Py/Pt structure. The presence of ANE has also been detected in all of the prepared thin films for the presence of perpendicular T gradient, ∇T_z , across the film plane due to the lower thermal conductivity of FM thin films compared to that of the MgO substrate. This unconventional ANE interrupts the signal of SSE and seems to be responsible for the asymmetric strength of V in the SSE measurement at HT and LT ends of the sample. The effect of this kind of artifact on the signal of SSE implies that considerable

attention should be given for future investigations. Moreover, this study suggests that the spin polarization of conduction electrons in ferromagnetic metal thin films does not dominate the mechanism of SSE.

ACKNOWLEDGMENTS

This work was supported by the Grant-in-Aid for Scientific Research in Priority Area “Creation and control of spin current” (Grant No. 19048004), and Young Scientists (B) (Grant No. 20760005) by MEXT, Japan. This work was a part of the cooperative research program of the Advanced Research Center of Metallic Glasses, Institute for Materials Research, Tohoku University. This work was also supported in part by Global COE Program “Materials Integration (International Center of Education and Research), Tohoku University,” MEXT, Japan.

*bosusj@imr.tohoku.ac.jp

¹M. N. Baibich, J. M. Broto, A. Fert, F. Nguyen Van Dau, F. Petroff, P. Eitenne, G. Creuzet, A. Friederich, and J. Chazelas, *Phys. Rev. Lett.* **61**, 2472 (1988).

²G. Binasch, P. Grünberg, F. Saurenbach, and W. Zinn, *Phys. Rev. B* **39**, 4828 (1989).

³S. A. Wolf, D. D. Awschalom, R. A. Buhrman, J. M. Daughton, S. von Molnár, M. L. Roukes, A. Y. Chtchelkanova, and D. M. Treger, *Science* **294**, 1488 (2001).

⁴C. Chappert, A. Fert, and F. N. V. Dau, *Nat. Mater.* **6**, 813 (2007).

⁵A. Fert, *Rev. Mod. Phys.* **80**, 1517 (2007).

⁶S. Takahashi, H. Imamura, and S. Maekawa, in *Concepts in Spin Electronics*, edited by S. Maekawa (Oxford University Press, Oxford, 2006).

⁷Spin Caloritronics, edited by G. E. W. Bauer, A. H. Macdonald, and S. Maekawa, special issue of *Solid State Commun.* **150**, 459 (2010).

⁸K. Uchida, S. Takahashi, K. Harii, J. Ieda, W. Koshibae, K. Ando, S. Maekawa, and E. Saitoh, *Nature (London)* **455**, 778 (2008).

⁹K. Uchida, S. Takahashi, J. Ieda, K. Harii, K. Ikeda, W. Koshibae, S. Maekawa, and E. Saitoh, *J. Appl. Phys.* **105**, 07C908 (2009).

¹⁰K. Uchida, T. Ota, K. Harii, S. Takahashi, S. Maekawa, Y. Fujikawa, and E. Saitoh, *Solid State Commun.* **150**, 524 (2010).

¹¹K. Uchida, T. Ota, K. Harii, K. Ando, K. Sasage, H. Nakayama, K. Ikeda, and E. Saitoh, *IEEE Trans. Magn.* **45**, 2386 (2009).

¹²K. Uchida, T. Ota, K. Harii, K. Ando, H. Nakayama, and E. Saitoh, *J. Appl. Phys.* **107**, 09A951 (2010).

¹³E. Saitoh, M. Ueda, H. Miyajima, and G. Tatara, *Appl. Phys. Lett.* **88**, 182509 (2006).

¹⁴J. Xiao, G. E. W. Bauer, K. C. Uchida, E. Saitoh, and S. Maekawa, *Phys. Rev. B* **81**, 214418 (2010).

¹⁵Iosif Galanakis and Peter H. Dederichs, in *Half-Metallic Alloys: Fundamentals and Applications (Lecture Notes in Physics 676)*, edited by I. Galanakis and P. Dederichs (Springer, Berlin, Heidelberg, 2005), pp. 1–39, and references therein.

¹⁶S. Fujii, S. Sugimura, S. Ishida, and S. Asano, *J. Phys. Condens. Matter* **2**, 8583 (1990).

¹⁷S. Picozzi, A. Continenza, and A. J. Freeman, *Phys. Rev. B* **66**, 094421 (2002).

¹⁸Y. Sakuraba, J. Nakata, M. Oogane, H. Kubota, Y. Ando, A. Sakuma, and T. Miyazaki, *Jpn. J. Appl. Phys.* **44**, L1100 (2005).

¹⁹Y. Sakuraba, M. Hattori, M. Oogane, Y. Ando, H. Kato, A. Sakuma, T. Miyazaki, and H. Kubota, *Appl. Phys. Lett.* **88**, 192508 (2006).

²⁰Y. Sakuraba, T. Iwase, K. Saito, S. Mitani, and K. Takanashi, *Appl. Phys. Lett.* **94**, 012511 (2009).

²¹T. Iwase, Y. Sakuraba, S. Bosu, K. Saito, S. Mitani, and K. Takanashi, *Appl. Phys. Express* **2**, 063003 (2009).

²²Y. Sakuraba, K. Izumi, T. Iwase, S. Bosu, K. Saito, K. Takanashi, Y. Miura, K. Futatsukawa, K. Abe, and M. Shirai, *Phys. Rev. B* **82**, 094444 (2010).

²³Y. Sakuraba *et al.* (unpublished).

²⁴B. Balke, S. Ouardi, T. Graf, J. Barth, C. G. F. Blum, G. H. Fecher, A. Shkabko, A. Weidenkaff, and C. Felser, *Solid State Commun.* **150**, 529 (2010).

²⁵T. Kimura, J. Hamrle, and Y. Otani, *Phys. Rev. B* **72**, 014461 (2005).

²⁶F. J. Jedema, M. S. Nijboer, A. T. Filip, and B. J. van Wees, *Phys. Rev. B* **67**, 085319 (2003).

²⁷A. A. Abdurakhmanov, E. S. Gravrilov, and A. R. Rasulov, *Izv. Vyssh. Uchebn. Zaved. Fiz.* **6**, 78 (1984) [*Sov. Phys. J.* **6**, 78 (1984)].

²⁸H. Watanabe, *Thermochim. Acta* **218**, 365 (1993).

²⁹K. Ando, Y. Kajiwara, K. Sasage, K. Uchida, and E. Saitoh, *IEEE Trans. Magn.* **46**, 1331 (2010).

³⁰K. Uchida, J. Xiao, H. Adachi, J. Ohe, S. Takahashi, J. Ieda, T. Ota, Y. Kajiwara, H. Umezawa, H. Kawai, G. E. W. Bauer, S. Maekawa, and E. Saitoh, *Nat. Mater.* **9**, 894 (2010).

³¹C. M. Jaworski, J. Yang, S. Mack, D. D. Awschalom, J. P. Heremans, and R. C. Myers, *Nat. Mater.* **9**, 898 (2010).

³²Y. Pu, E. Johnston-Halperin, D. D. Awschalom, and J. Shi, *Phys. Rev. Lett.* **97**, 036601 (2006).

³³M. Hatami, G. E. W. Bauer, S. Takahashi, and S. Maekawa, *Solid State Commun.* **150**, 480 (2010).